MORPHOLOGICAL AND SURFACE ASPECTS OF CELLULOSE-LIGNIN HYDROGELS

DIANA CIOLACU, FLORICA DOROFTEI, GEORGETA CAZACU and MARIA CAZACU

"Petru Poni" Institute of Macromolecular Chemistry,
41A, Grigore Ghica Voda Alley, Iasi, Romania

Received September 24, 2012

Cellulose-lignin hydrogels (CL), prepared by a two-step procedure consisting in dissolving the cellulose in an alkaline solution at low temperature, followed by the crosslinking reaction with lignin in the presence of epichlorohydrin, were subjected to experimental approaches, additional to those reported before, for their in-depth characterization. Thus, the morphology was examined by optical and scanning electron microscopy (SEM), while some surface properties (surface area, average pore size, and sorption capacity) were estimated by dynamic water vapor sorption (DVS) analysis. The changes in crystalline structure of the samples were confirmed by X-ray diffractometry (XRD). It has been found that these characteristics are influenced by the lignin whose presence leads to increased porosity of the material.

Keywords: cellulose-lignin hydrogel, dynamic water vapor sorption, X-ray diffraction, optical microscopy, scanning electron microscopy, structural characterization

INTRODUCTION

Cellulose is the major extracellular matrix component of plant cells and the most abundant naturally occurring biopolymer.[1] From the point of view of the molecular structure, cellulose is a linear homopolymer composed of units of anhydro-β-D-glucopyranose (AGU), linked together by β(1→4)-glycosidic bonds. Due to its renewability, biodegradability and low cost, cellulose presents increasing interest for a large number of biomedical and pharmaceutical applications. Thus, cellulose-based materials are the major pharmaceutical excipients, utilized in drug delivery dosage forms, and have wide application in tissue engineering, as wound healing, artificial kidney, artificial blood vessels, bone, cartilage and cardiovascular tissue engineering.[2] Cellulose-based hydrogels are of high interest for such applications and can be obtained via either physical or chemical stabilization of aqueous solutions of cellulosics. The chemically crosslinked hydrogels are obtained using difunctional molecules as crosslinkers, which covalently bind different polymer molecules in a three-dimensional hydrophilic network. Epichlorohydrin, aldehydes and aldehyde-based reagents, urea derivatives, carbodiimides and multifunctional carboxylic acids are the most widely used crosslinkers for cellulose.[3,4] These materials are capable to retain a large amount of water and because of their soft and rubbery consistence, closely resemble living tissues. Another important natural polymer is lignin – a renewable, amorphous biopolymer consisting of phenylpropane units linked together through various types of ether- and carbon-carbon bonds to form a polymer lacking regularity, crystallinity, or optical activity. It is an important constituent of various plants and is, among the naturally occurring polymers, second to cellulose in natural abundance.[5] Recently, potential health benefits have been attributed to lignin, such as antioxidant properties, as well as antibacterial, antitumoral, antiviral, and immunopotentiating activity.[6-8] It has been found that lignin displayed potent antiviral activity by directly interacting with the virus. Anti-HIV activity of lignin was significantly higher than that of tannins and flavonoids.[9] Recently, we have reported the preparation of new cellulose-lignin hydrogels, in order to combine the biocompatibility with tissues and blood, non-toxicity and low price of cellulose with the antioxidant property of lignin, with the aim of testing in cosmetic and pharmaceutical applications.[10]

In this paper, we provide some additional information, i.e. the morphology, porosity, surface area and pore size distribution, which are discussed in correlation with the hydrogel composition. The investigations on these hydrogels have been performed by X-ray diffraction (XRD) and dynamic water vapor sorption (DVS) analyses and by optical and scanning electron microscopy (SEM).

EXPERIMENTAL

Materials

Microcrystalline cellulose, Avicel PH-101 (Fluka) and steam explosion lignin from aspen wood (ENEA, Italy) were used in order to obtain new hydrogels based on natural polymers.

Cellulose hydrogel (C) and cellulose-lignin hydrogels (CL) were prepared according to the procedure described by Ciolacu *et al.*[10] Thus, hydrogel C was prepared in a two-step method, consisting in dissolving 0.5 g microcrystalline cellulose in 6.7 mL solution of 8.5% NaOH, by freezing at low temperature (-30 °C), followed by the crosslinking reaction for 8 h at 80 °C, in the presence of 2.14 mL epichlorohydrin. The hydrogels were then washed with warm and cold distilled water, during ten days, in order to remove the NaOH in excess, the NaCl formed and the epichlorohydrin traces. The samples were dried in a freeze-dryer.

For the preparation of cellulose/lignin hydrogels, the cellulose was firstly dissolved in alkaline solution at low temperature, as described above. To the obtained cellulose solution, different amounts of lignin (3:1, 2:1, 1:1, 1:2, 1:3, as gravimetric ratios) and then 2.14 mL epichlorohydrin were added under continuous stirring. The crosslinking reactions were performed for 8 h, at 80 °C and then the hydrogels were washed thoroughly with warm and cold water and were dried in a freeze-dryer.

Equipments

Dynamic vapor sorption (*DVS*): Dynamic water vapors sorption capacity of the cellulose-lignin hydrogels was measured in the dynamic regime using IGAsorp, a fully automated gravimetric analyzer, supplied by Hiden Analytical, Warrington (UK). This equipment contains an ultrasensitive microbalance with a 0.1 μg resolution for 100 mg range and a 200 mg capacity, and registers the weight changes as the humidity is modified in the sample chamber, at a constant regulated temperature.

X-ray diffraction analysis (*XRD*): The X-ray diffraction was performed on a Bruker-AXS: D8 ADVANCE apparatus, equipped with a transmission type goniometer using Ni-filtered, Cu-Kα radiation at 40 kV. The goniometer was scanned stepwise every 0.10° from 10 to 40° in the 2θ range. The resulting diffraction patterns exhibited peaks that were deconvoluted from a background scattering by using Lorenzian functions, while the diffraction pattern of an amorphous sample was approximated by a Gaussian function curve fitting analysis.[11,12]

Optical microscopy: The aspect of the samples has been examined with Leica DM 2500 M optical microscope in polarized light, at room temperature and a magnification of 50x.

Scanning electron microscopy (*SEM*): The morphology of the samples was investigated by using a Quanta 200 type scanning electron microscope, operating at 30 kV with secondary electrons, in low vacuum mode. For a better observation of the pores, the hydrogels were previously freeze-dried in an ALPHA 1-2/LD device (Martin Christ GmbH, Germany), for 15 hours, at -65 °C. The cross-sections were prepared by cutting the dry hydrogels with a sharp razor blade, in order to expose the internal structures.

RESULTS AND DISCUSSION

A series of hydrogels (Table 1) were prepared by a new two-step procedure consisting in dissolving the cellulose in an alkaline solution at low temperature, followed by the crosslinking reaction with lignin in the presence of epichlorohydrin, as described previously.[10]

Table 1
Compositions and maximum swelling degree of the prepared hydrogels[10]

Sample	Cellulose/lignin feed mass ratio	Qmax, %
C	1:0	1145
CL_1	3:1	2358
CL_2	2:1	2446
CL_3	1:1	2642
CL_4	1:2	2737
CL_5	1:3	3061

C:L = 1:1 C:L = 1:3

a b

Figure 1: Photo images of CL hydrogels with different compositions: a) CL3; b) CL5

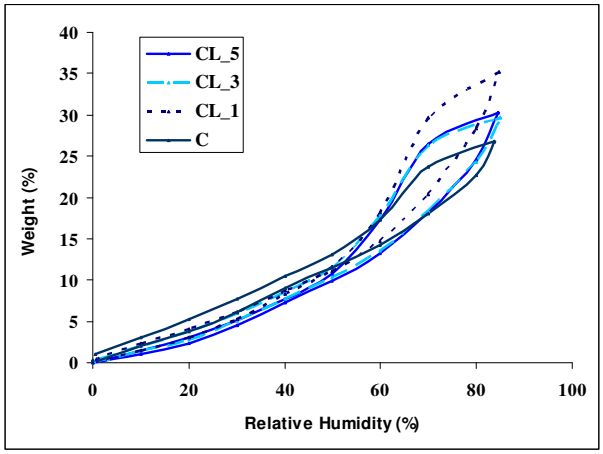

Figure 2: Sorption/desorption isotherms for cellulose-lignin hydrogels (CL_1, CL_3 and CL_5), as compared with that of cellulose-based hydrogel (C)

The swelling degree of the hydrogels in distilled water was determined gravimetrically, using the following relation:

$$Q\max = \frac{m - m_0}{m_0} \cdot 100 \ (\%) \qquad (1)$$

where: m_0 – dried hydrogel weight, g;
m – swollen hydrogel weight, g.

The aspect of the samples after purification with warm and cold distilled water is shown in Figure 1. The color of the samples changes from light to dark brown, as the incorporated lignin amount increases. It appears that the structure is uniform and densely packed.

These hydrogels have already been characterized by different methods: UV-VIS and FT-IR spectroscopy, DSC and SEM.[10] It has been found that the swelling degree of these hydrogels rises with the increase of the lignin content, from sample C (1145%) to CL_5, which has the highest value (3061%), which demonstrates the superabsorbant character of these types of hydrogels.

In this paper, the samples were subjected to additional experimental investigations for their in-depth characterization.

Dynamic water vapor sorption analysis (DVS)

Many of the useful properties of the biomaterials for medical applications are related to their sorption and swelling capacity for water.[13] In order to study the behavior of the prepared hydrogels in the presence of humidity, water vapor sorption capacity was measured at 25 °C in the 0-90% relative humidity range (RH) in the dynamic regime.

The dynamic water vapor sorption analysis (DVS) is a precise method used to establish the interactions that take place between the hydrogels and water, with a perspective over the future application performance. The drying of the hydrogels before sorption measurements was carried out at 25 °C in flowing nitrogen until the weight of the sample reached equilibrium at RH <1%, which is considered the dry mass. After drying, the measurements began with the sorption

curve. The vapor pressure was increased in 10% humidity steps, each having a pre-established equilibrium time between 20 and 25 minutes. At each step, the weight gained was measured by electromagnetic compensation between tare and sample when equilibrium was reached. After the maximum level for RH was reached, the desorption step began and the cycle was ended by decreasing the vapor pressure until the desorption isotherm was obtained. The sorption/desorption isotherms registered for three of the samples, as compared with cellulose hydrogel as reference, are presented in Figure 2.

According to the earlier studies reported in literature, water sorption on cellulose is a two-stage process.[20] The first stage is a water diffusion rate-controlling process, while in the second stage, the rate is governed by a relaxation mechanism. All isoterms can be considered of type III, according to Brunauer *et al*.,[14] indicating that the results should not be described in terms of free and bound water and of hydration layers. The isotherms of cellulose-lignin show hysteresis between the adsorption and desorption cycle at RH > 60%, this being usually attributed to pore effects.[15] The cellulose hydrogel also shows slight hysteresis in the low and medium RH levels, which is the effect of the crystallinity degree. Classical explanations of hysteresis are based on a change in geometry during the adsorption and desorption processes.[15] According to the IUPAC classification of the hysteresis, in our case it can be assimilated with H2 type. In a simplified manner, this shape of the hysteresis is generally attributed to a difference in mechanism between condensation and evaporation processes occurring in pores with narrow necks and wide bodies, but it is believed that network effects have an important role.[16]

The Brunaeur-Emmet-Teller (BET) model based on the equation:[14]

$$W = \frac{W_m \cdot C \cdot RH}{(1-RH)\cdot(1-RH+C\cdot RH)} \quad (2)$$

where: W – the weight of adsorbed water;
W_m – the weight of water forming a monolayer;
C – the sorption constant;
RH – the relative humidity,
was used for modeling the sorption isotherms and evaluating the surface area based on the water vapor sorption data registered in the conditions presented in Experimental section.[14] The sorption values for water activities between 0.05-0.35 were considered, where BET equation is applicable with good results. In order to estimate the average pore size, the model of Barett, Joyner and Halenda (BJH model) was applied considering pores to be cylindrical.[14,17] The method uses the desorption branch of the isotherm, where either the evaporation of the liquid core or the desorption of a multilayer occurs.

The relationship between the liquid volume V_{liq} and the percentage uptake n, is the following:

$$V_{liq} = \frac{n}{100 * \rho_a} \quad (3)$$

where: V_{liq} – the liquid volume, mL;
n – the percentage uptake, %;
ρ_a – the adsorbed phase density, kg/m^3.

The average pore size can be calculated from the pore volume assuming cylindrical pore geometry.

$$r_{pm} = \frac{2 \cdot V_{liq}}{A} \quad (4)$$

where: r_{pm} – the average pore size, nm;
V_{liq} – the liquid volume, mL;
A – the BET surface area, m^2/g.

From equations (3) and 4), relation (5) is obtained:

$$r_{pm} = \frac{2 \cdot n}{100 \cdot \rho_a \cdot A} \quad (5)$$

The surface parameters calculated based on sorption/desorption isotherms are summarized in Table 2.

Examining the data regarding the surface parameters of hydrogels, it can be seen that the presence of lignin in the structure of the hydrogel increases the maximum water vapor sorption capacity from 23.5 wt% in simple cellulose hydrogel up to 32.1 wt% in the CL_3 hydrogel, in which the cellulose:lignin mass ratio is 1:1. This behavior could be explained by the relaxation of the hydrogel's networks due to the presence of lignin, reflected in a higher swelling capacity, as previously demonstrated.[10] Thus, during the cellulose crosslinking, a part of its OH groups are consumed in the reaction, reducing the water accessibility. When lignin is added to cellulose and they are co-crosslinked, they both participate with functional groups in this reaction. Therefore, as the lignin content in the hydrogel rises, some hydroxyl groups are blocked by forming C-O-C linkages, while many other remain free, which favours water sorption. This happens up to a certain point beyond which the hydrophobic

character of lignin becomes dominant. In addition, in all cases, as a result of the crosslinking with epichlorohydrine, new OH groups are formed by epoxide ring opening.

The average pore size (r_{pm}) determined from the desorption branch lies in the 2.09-3.15 nm range, slightly higher as compared to that estimated (1.66 nm) in the case of simple cellulose hydrogel. This might be justified by the complexity of factors that may have opposite effects on surface properties of these hydrogels (chemical crosslinking degree, the presence of polar groups and hydrogen bonding degree, pore shape, sorption type, etc.). Similarly, the BET area values are close to those determined for cellulose gel. Other characteristics (humidity loss and drying rate) of the desorption process were estimated by using eqs. (6) and (7) and are presented in Table 3.

The humidity loss (ΔW, %) was determined with the following equation:

$$\Delta W = \frac{m - m_0}{m_0} \cdot 100 \ (\%) \qquad (6)$$

where: m – the weight at a relative humidity of 90%, g;

m_0 – the weight at a relative humidity of 0%, g,

while the drying rate (η, %/s) was calculated with the formula:

$$\eta = \frac{\Delta W}{\Delta t} \cdot 10^3 \ (\%/s) \qquad (7)$$

where: ΔW – the humidity loss, %;

Δt – the period of time, s.

As expected, the higher the amount of absorbed water, the greater the humidity loss (ΔW). The same tendency can be noticed for the drying rate (η, %/s), this proportionality supporting the hypothesis that the desorption mechanism is the same in all cases.

X-ray diffraction analysis

In order to identify the structural modifications taking place within hydrogels by increasing the amount of the lignin from the cellulose matrix, the deconvolution of the peaks was performed using a soft PeakFit 4.11.

Table 2
The main surface parameters calculated based on water vapors sorption/desorption isotherms

Sample	Sorption capacity, %	Sorption branch			Desorption branch		
			BET		BET		
		r_{pm}, nm	Area, m^2/g	Monolayer, g/g	Area, m^2/g	Monolayer, g/g	r_{pm}, nm
C	23.5	1.42	332	0.094450	282	0.080482	1.66
CL_1	27.9	2.10	265	0.075513	266	0.075861	2.09
CL_3	32.1	3.38	190	0.054260	240	0.068378	2.68
CL_5	25.4	1.03	492	0.140031	161	0.045970	3.15

Table 3
Main desorption parameters of C and CL hydrogels

Sample	m_0 (mg)	m (mg)	ΔW (%)	t_{final} (s)	η (%/s)
C	5.37	6.46	20.27	2404	8.43
CL_1	4.47	5.61	25.50	3168	8.05
CL_3	1.63	2.29	40.79	4297	9.49
CL_5	3.66	4.56	24.62	2887	8.53

One would have expected the X-ray diffractograms of the hydrogels to be very similar to that of cellulose II, because cellulose in the presence of NaOH solution and at high temperature is transformed in the allomorphic form of cellulose II. Generally, the diffractogram of cellulose II contains the characteristic crystal lattices with the maximum intensities at the peaks $(10\bar{1})$ and (002) at around 20º and 22º, respectively, while the peak (101) appears at a Bragg angle of 11°.[18]

Figure 3 presents comparatively the diffractograms for the allomorphic form of cellulose II obtained from microcrystalline cellulose, cellulose-based hydrogel, and cellulose-lignin hydrogels.

X-ray studies confirm that the bi-component hydrogels undergo distinct transformations by

increasing the lignin content. An important decrease of all intensities characteristic of the main crystallographic peaks, but especially of the intensity of (020) lattice diffractions was recorded. This observation confirms the hydrogel formation between cellulose and lignin, because the contribution of lignin, an amorphous natural polymer, determines the decrease of the crystallinity of the samples.

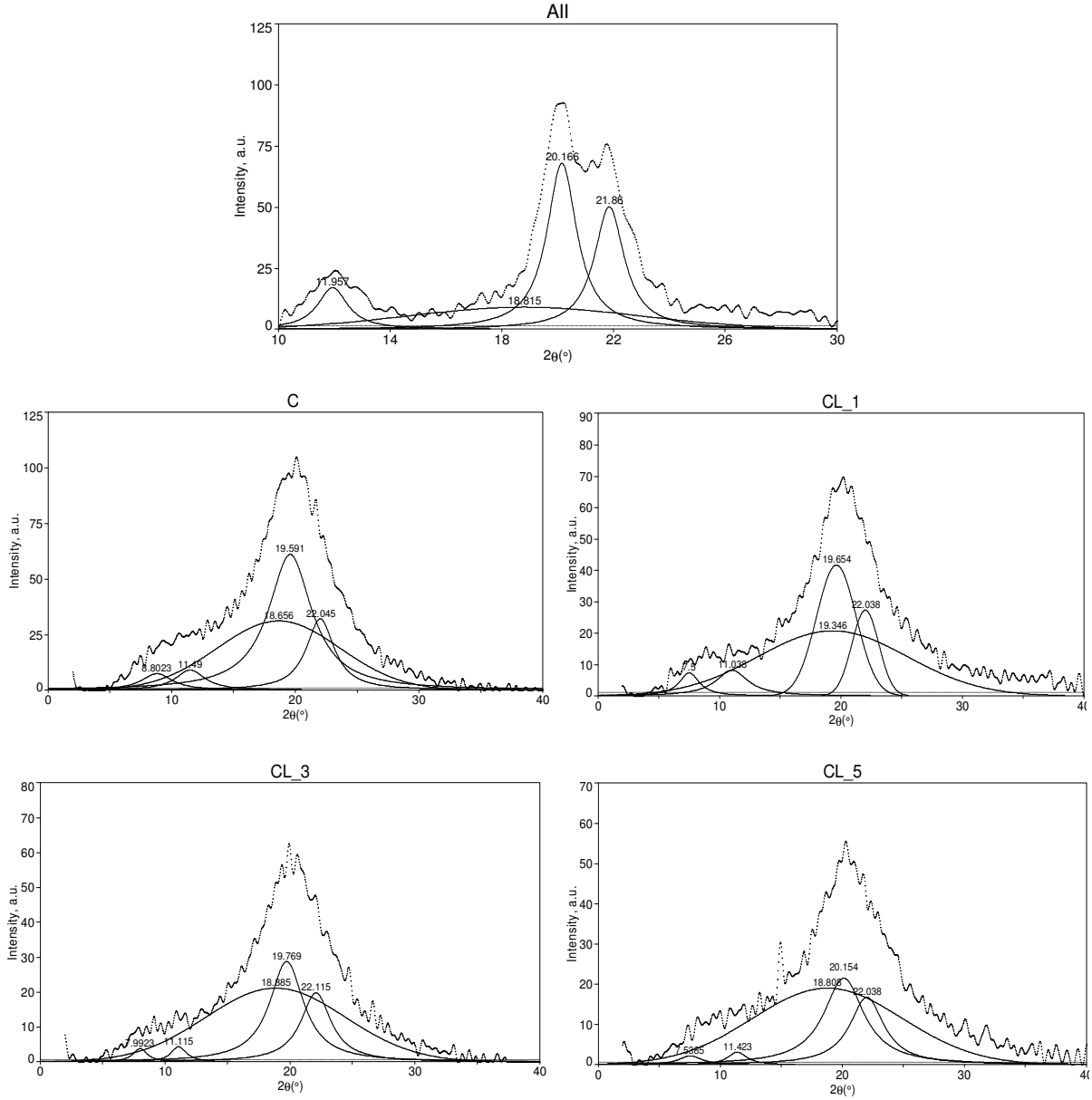

Figure 3: X-ray diffractograms of microcrystalline cellulose II (AII), cellulose hydrogel (C), cellulose-lignin hydrogels (CL_1, CL_3 and CL_5)

Table 4 summarizes the changes in the crystalline structure of the cellulose-based hydrogel and of cellulose-lignin hydrogels. The crystallinity index (CrI) of the hydrogels was established by the following equation:[19]

$$Cr.I. = [Ac/(Aa+Ac)] \cdot 100\ (\%) \quad (8)$$

where: Ac – the surface of the crystalline area, m^2;

Aa – the surface of the amorphous area, m^2.

The crystallinity index (CrI) decreased constantly from 61.6%, corresponding to cellulose-based hydrogel (C), to 46.7%, value characteristic of hydrogels obtained from cellulose-lignin with a ratio of 1:1, and further to 45.2% for CL_5 hydrogel.

Optical microscopy

The optical micrographs of cellulose-lignin based hydrogels (CL) are presented in Figure 4. It can be seen that the average pore size of hydrogels increases as lignin content increases, which suggests that a higher quantity of water can be uptaken, this assumption being in good agreement with the data obtained for swelling degree and the DVS data for the hydrogels.

Scanning electron microscopy (SEM) analysis

SEM images provide information regarding the pore and size geometry, as well as relevant information regarding the homogeneity or heterogeneity of the hydrogel network. Some additional cross-section images to those already shown[10] for hydrogels obtained from cellulose (C) and from different ratios of cellulose and lignin (CL) are presented in Figure 5.

Table 4
Characteristic diffraction angles of the main crystal lattices and crystallinity index for the studied samples

Samples	CrI, %	Diffraction angle, 2θ, °		
		101	$10\bar{1}$	002
AII	77	11.9	20.1	21.8
C	61.6	11.5	19.6	22
CL_1	49.4	11.0	19.6	22
CL_3	46.7	11.1	19.7	22
CL_5	45.2	11.4	20.1	22

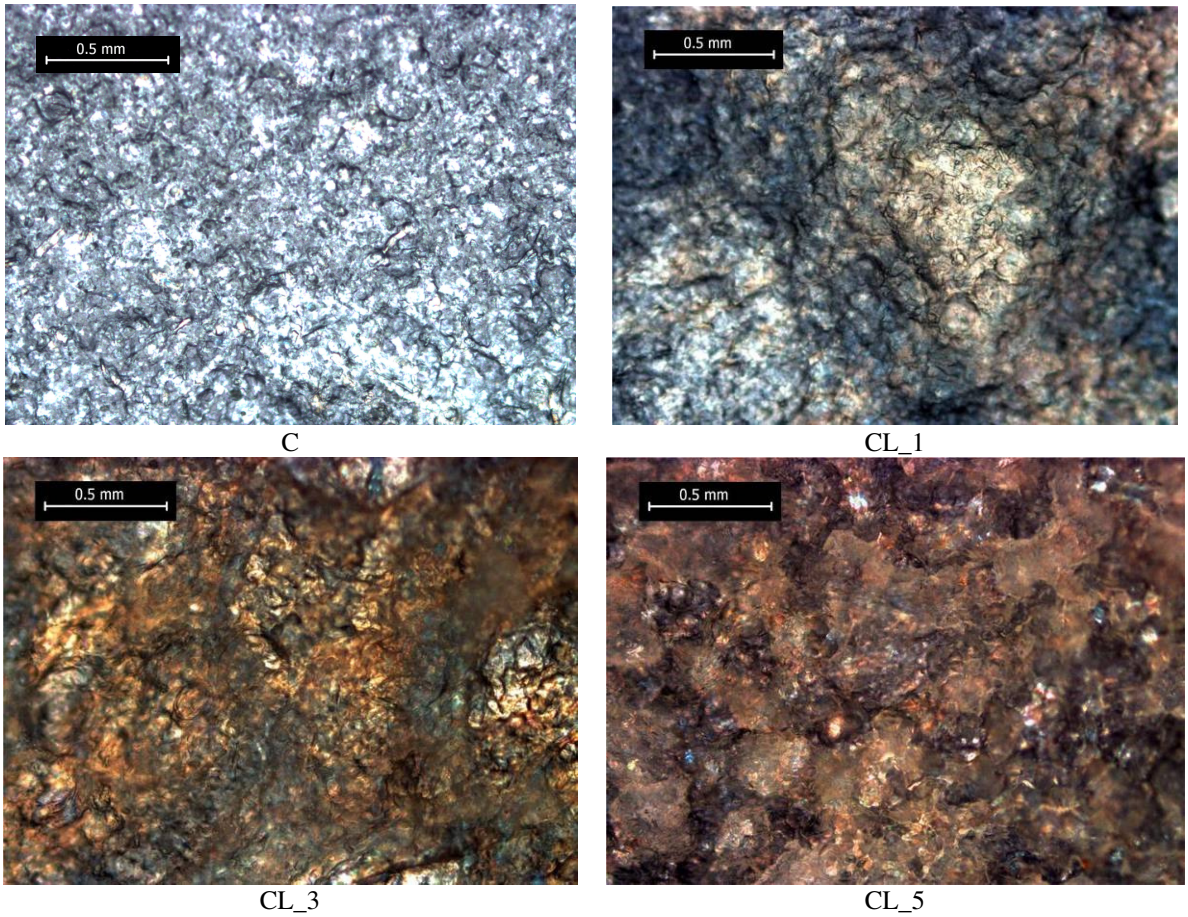

C CL_1

CL_3 CL_5

Figure 4: Optical photographs of hydrogels based on cellulose (C) and cellulose-lignin (CL)

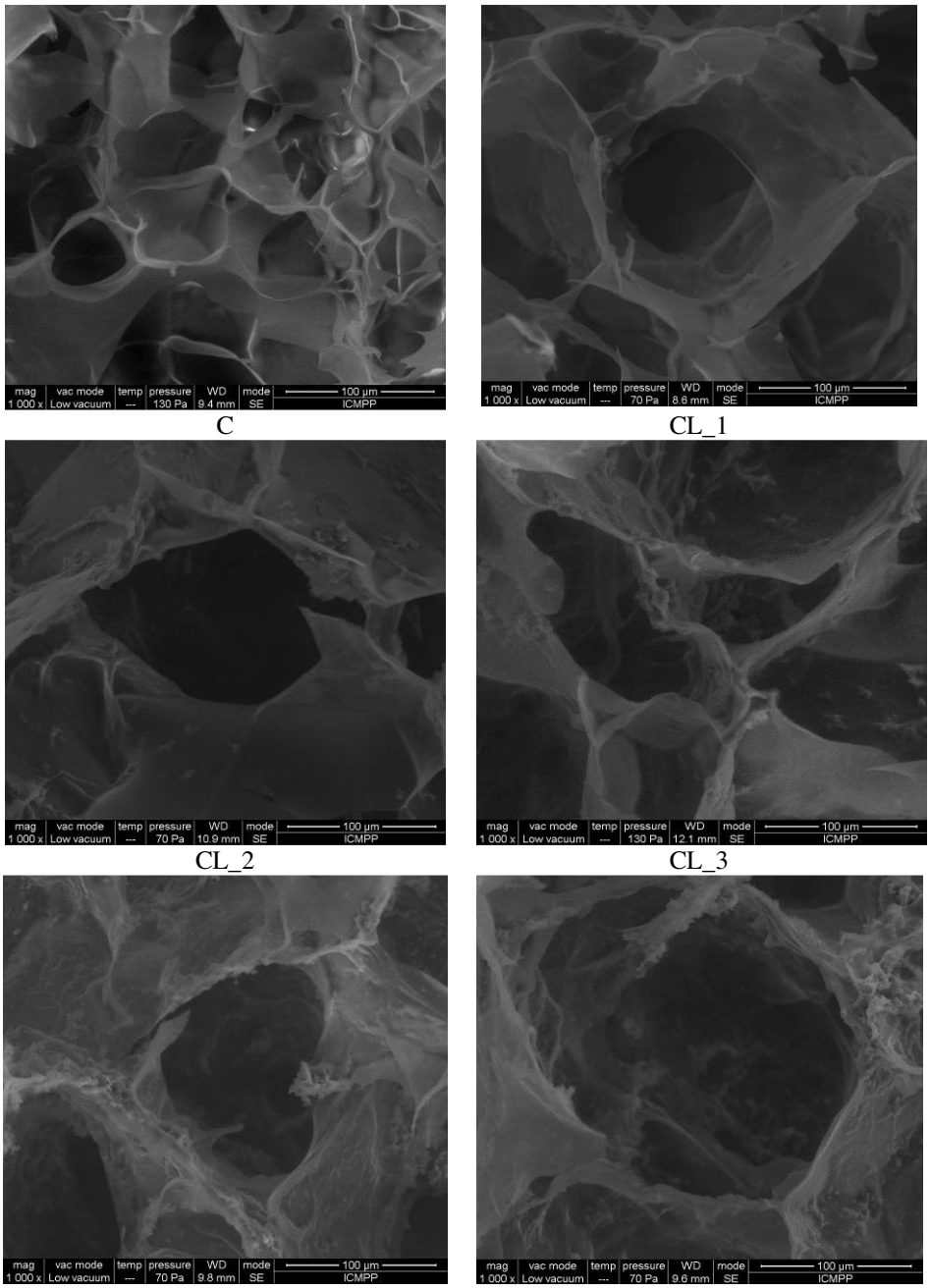

Figure 5: SEM images of different cellulose and cellulose-lignin hydrogels

The average pore size of the cellulose hydrogels estimated on the basis of SEM images (Table 5) indicates a macro-porous structure with pore sizes between 169 (C) and 431 μm (CL_5). These values are much higher than those estimated from water vapor sorption analysis, which is a much more in-depth analysis. The pores estimated by the previous procedure are in fact in the walls of the pores revealed by optical and electronic procedures. It can be observed that the average pore size of the hydrogels increased with the rise of the lignin content, which is in agreement with the data obtained from the swelling degree of the hydrogels and from the optical microscopy analysis. An explanation for this behavior is the fact that the incorporation of a higher amount of lignin in the network, owing to a bulky and branched structure, contributes to an increase of ether linkages and implicitly to an increase of the swelling degree of the hydrogels.

Figure 6 shows the pore size distribution for cellulose-lignin hydrogels. It can be observed that the hydrogels with a high amount of lignin exhibit

a broader pore size distribution than the ones with small quantity of lignin.

Table 5
The pore dimensions estimated based on SEM images

Sample	Average pore size, μm
C	169
CL_1	203
CL_2	215
CL_3	233
CL_4	307
CL_5	431

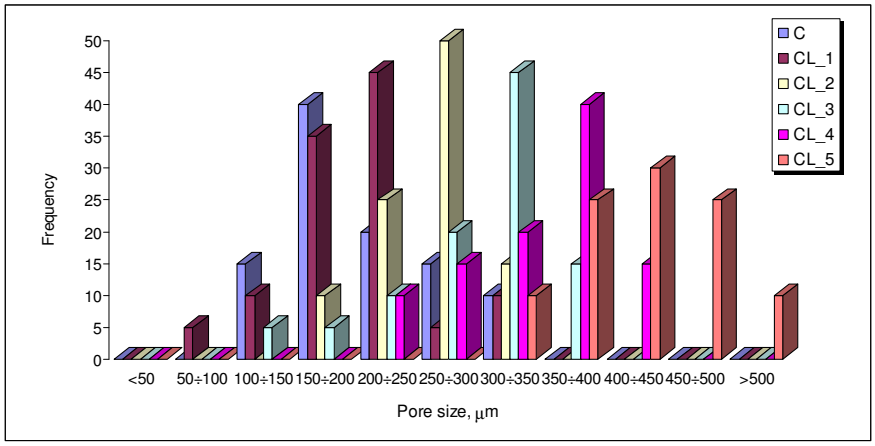

Figure 6: Pore size distribution of cellulose-lignin hydrogels

From the resulted data, it can be concluded that the ratios of the hydrogel components significantly influence the hydrogel pore size, as well as pore size distribution. Thus, by increasing the amount of lignin in the cellulose matrix, the pore size distribution becomes wider and the share of large pores increases. Such a suggestion confirmed the data obtained from the swelling measurements, showing that the increase of lignin in the CL hydrogels permits a higher water uptake.

CONCLUSION

The incorporation of lignin in a co-network with cellulose by crosslinking leads to a colored product, the intensity of the effect depending on the lignin content. The morphology of the samples revealed through optical or SEM images indicated a macro-porous structure, with pore sizes between 169 and 431 μm in diameter, increasing with the lignin content. The values are much higher than those estimated from water vapor sorption analysis (3.54-5.50 nm), which is a much more in-depth analysis. The lignin presence also induces an increase in water vapor sorption capacity, but this dependence is more complex than in the case of the derived parameters (BET area and pore size). The increase of lignin content also determines a decrease of the crystallinity index, from 61.6% to 45.2%, as established by X-ray diffraction analysis.

ACKNOWLEDGEMENTS: This research was financially supported by the European Social Fund – "Cristofor I. Simionescu" Postdoctoral Fellowship Programme (ID POSDRU/89/1.5/S/55216), Sectorial Operational Programme for Human Resources Development 2007–2013.

REFERENCES

[1] S. Kamel, N. Ali, K. Jahangir, S. M. Shah and A. A. El-Gendy, *eXPRESS Polym. Lett.*, **2**(**11**) 758 (2008).
[2] Z. Yue, F. Wen, S. Gao, M. Y. Ang, P. K. Pallathadka, L. Liu and H. Yu, *Biomaterials*, **31**(**32**), 8141 (2010).
[3] A. Sannino, C. Demitri and M. Madaghiele, *Materials*, **2**, 353 (2009).

[4] C. Demitri, R. Del Sole, F. Scalera, A. Sannino, G. Vasapollo *et al*., *J. Appl. Polym. Sci*., **110**(**4**), 2453 (2008).
[5] W. K. El-Zawawy, *Polym. Adv. Technol*., **16**, 48 (2005).
[6] M. Mitjans and M. P. Vinardell, *Trends Comp. Biochem. Physiol*., **11**, 55 (2005).
[7] V. Ugartondo, M. Mitjans and M. P. Vinardell, *Ind. Crop. Prod*., **30**, 184 (2009).
[8] K. Toh, H. Yokoyama, H. Noda and Y. Yuguchi, *J. Food Biochem*., **34**(**1**), 192 (2010).
[9] J. N. Thakkar, V. Tiwari and U. R. Desai, *Biomacromolecules*, **11**(**5**), 1412 (2010).
[10] D. Ciolacu, A. M. Oprea, N. Anghel, G. Cazacu and M. Cazacu, *Mat. Sci. Eng. C*, **32**, 452 (2012).
[11] D. Ciolacu, *J. Optoelectron. Adv. Mater*., **9**(**4**), 1033 (2007).
[12] D. Ciolacu and V. I. Popa, "Cellulose Allomorphs: Structure, Accessibility and Reactivity", Nova Science Publishers, Inc., United States, 2010.
[13] S. Chen, J. Hu and H. Zhuo, *J. Mater. Sci*., **46**(**20**), 6581 (2011).
[14] S. Brunauer, L. S. Deming, W. E. Deming and E. Teller, *J. Am. Chem. Soc*., **62**(**7**), 1723 (1940).
[15] L. Zhou, Thesis for Degree of Master of Science, The University of Minnesota, 2010.
[16] IUPAC Recommendations, *Pure Appl. Chem*., 57603 (1985).
[17] K. L. Murray, N. A. Seaton and M. A. Day, *Langmuir*, **15**, 6728 (1999).
[18] D. Ciolacu, L. Pitol-Filho and F. Ciolacu, *Cellulose*, **19**, 55 (2012).
[19] Y. Sun, J. Zhuang, L. Lin and P. Ouyang, *Biotechnol. Adv*., **27**, 625 (2009).
[20] C. Newns, *Trans. Faraday Soc*., **52**, 1533 (1956).